

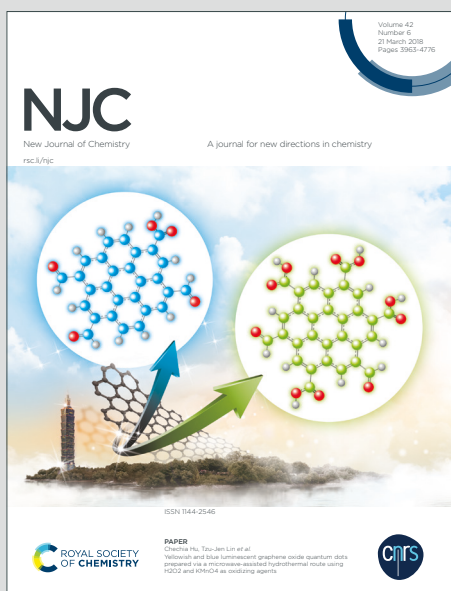
NJC

New Journal of Chemistry

A journal for new directions in chemistry

Accepted Manuscript

This article can be cited before page numbers have been issued, to do this please use: M. Arumugam, K. Paul Reddy, R. S. Meerakrishna, B. Satpati and P. Shanmugam, *New J. Chem.*, 2020, DOI: 10.1039/D0NJ04255B.



This is an Accepted Manuscript, which has been through the Royal Society of Chemistry peer review process and has been accepted for publication.

Accepted Manuscripts are published online shortly after acceptance, before technical editing, formatting and proof reading. Using this free service, authors can make their results available to the community, in citable form, before we publish the edited article. We will replace this Accepted Manuscript with the edited and formatted Advance Article as soon as it is available.

You can find more information about Accepted Manuscripts in the [Information for Authors](#).

Please note that technical editing may introduce minor changes to the text and/or graphics, which may alter content. The journal's standard [Terms & Conditions](#) and the [Ethical guidelines](#) still apply. In no event shall the Royal Society of Chemistry be held responsible for any errors or omissions in this Accepted Manuscript or any consequences arising from the use of any information it contains.

ARTICLE

Rapid Gram-Scale Synthesis of Au/Chitosan Nanoparticles catalysts by Using Solid Mortar Grinding

K. Paul Reddy^a, R. S. Meerakrishna^b, P. Shanmugam^b, Biswarup Satpati^c and A. Murugadoss^{*a}Received 00th January 20xx,
Accepted 00th January 20xx

DOI: 10.1039/x0xx00000x

Owing to the abundant functional groups present in the chitosan polymer, high density catalytic tiny gold particles with greater dispersion can be anchored on chitosan powder by using simple mortar and pestle. Chitosan supported gold nanoparticles (NPs) with excellent control of size and shape has been synthesized rapidly in gram-scale by solid-grinding without the need of any toxic solvents. The structure of the catalysts and products was established by advanced instrumental and spectroscopic methods. The supported gold NPs possesses as heterogeneous catalyst for the homocoupling of phenylboronic acid and the aerobic oxidation of benzyl alcohol in water. The catalytic behaviour and activity of the supported gold NPs was tuned/modulated by varying the ratio of chitosan polymer and gold precursor. Comparative studies showed that the solid chitosan supported gold catalyst exhibits superior catalytic activity and selectivity than the well known hydrophilic polymers stabilized gold NPs catalysts prepared by conventional solution based methods.

Introduction

The gram scale synthesis of highly stable with excellent size and shape controllability of gold nanoparticles (NPs) catalysts is continuing as one of the attractive research areas in various fields of science and technology, specifically in catalysis¹⁻⁴. The unique catalytic performance of polymer protected nanogold catalysts has been demonstrated in a number of chemical transformations such as alcohol oxidations⁵⁻⁷, carbon-carbon bond formation reactions⁸⁻¹⁰, and hydrogenations¹¹ etc. In the last two decades, various hydrophilic functional polymers such as poly vinyl alcohols, thiol linked polyethylene glycol, poly vinyl 2-pyrrolidone, starch, and cellulose have been used as stabilizers as well as capping agents for the synthesis of well-defined size and shape tuneable colloidal nanogold catalysts¹²⁻¹⁷. In contrast to solid metal oxide support, this hydrophilic polymers act as a catalytically inert stabilizer by multiple coordination sites, which weakly bound to gold NPs surface without affecting the intrinsic chemical properties of gold. Multifunctional groups present in the hydrophilic polymers have also potential to control both catalytic activity by donating the electronic charge and selectivity by activating the substrates during the catalytic reactions¹⁸⁻¹⁹.

These unique features make the colloidal nanogold as promising model catalysts for fundamental studies of heterogeneous catalysis.

Although significant progresses have been made for the synthesis of such polymers stabilized colloidal nanogold catalysts, these methodologies are mostly solution-based synthetic procedures, which are complex, tedious, consume large amounts of solvents²⁰. In addition, these solution-based methods are always slow in progress of nanogold catalysts based technologies and difficult to scale-up for laboratory/ industrial synthetic procedures²¹⁻²³. Another important constraint in the solutions-based approaches using functional polymers as a protective matrix is severely restricts in both scaling-up process and catalysis²⁴⁻²⁷. Due to their inherent viscous nature, it not only requires multiple purifications/ washing processes with excessive solvents, but also needed sophisticated equipment for purifications and drying to obtain the polymer protected colloidal nanogold catalysts^{24-25,28}. In addition, high loading of catalytically active gold NPs with good dispersion is always crucial to achieve excellent catalytic performance in the functional polymer stabilized nanogold catalysts using solution-based methods. Therefore, it is highly desirable to develop an alternative strategy that can overcome these drawbacks for the gram-scale preparation of the hydrophilic functional polymer supported gold NPs.

Chitosan is β -1,4-linked poly(d-glucosamine) derived from partial deacetylation of chitin²⁹⁻³⁰. In contrast to other hydrophilic functional polymers, chitosan is an inexpensive, highly stable solid polymer with rich multifunctional groups

^a Department of Inorganic Chemistry, University of Madras, Guindy Campus, Chennai – 600025, India. E-mail: murugadoss@unom.ac.in

^b Organic and Bioorganic Chemistry Division, Council of Scientific and Industrial Research (CSIR) – Central Leather Research Institute (CLRI), Adyar, Chennai – 600020, India.

^c Surface Physics and Material Science Division, Saha Institute of Nuclear Physics, Kolkata – 700064, India.

+ Electronic Supplementary Information (ESI) available: More TEM images, XPS, XANES and Langmuir-Isotherm plots for supported gold catalysts. Experimental procedure and reproduced spectra of products. See DOI: 10.1039/x0xx00000x

ARTICLE

Table 1. Content of gold before and after reduction (determined by ICP-OES), gold loading on chitosan supports (^aglucosamine monomer unit), and their effective surface area (^bdetermined from Langmuir-adsorption isotherm) and particles sizes of gold NPs supported on solid chitosan.

Sample name	Initial amount of gold (mmol)	Amount of chitosan (mmol) ^a	Gold loading (wt %)	Mole ratio of gold and chitosan ^a	Particle size (nm)	Effective surface area (m ² /g) ^b	Amount of Au from ICP-OES (mmol)
Chit-Au1	0.02	0.84	2.4	1:42	5.6±1.5	5.5 × 10 ³	0.0198
Chit-Au2	0.1	0.84	12.5	1:8	9.5±2.7	1.5 × 10 ³	0.0981
Chit-Au3	0.02	4.2	0.47	1:210	3.8±1.7	4.9 × 10 ³	0.0195
Chit-Au4	0.02x5	0.84x5	2.4	1:42	2.8±1.7	2.8 × 10 ⁴	0.0197

possesses great potential as an excellent support for metal cluster catalysts^{31–34}. For example, Ag NPs can be supported on solid chitosan which was subsequently used for the synthesis of bimetallic Au-Ag alloy NPs, where the chitosan powder used as both reducing as well as stabilizer for Ag and Au-Ag alloy NPs. Contrary to the solution-based processes, gram-scale quantity of solid chitosan supported Au-Ag alloy NPs catalysts can be synthesized by mortar grinding³⁵. Because of the weak reducing nature of chitosan, it is incapable to synthesize other noble metal NPs such as palladium and gold NPs by solid grinding. On the other hand, the gram-scale syntheses PVP stabilized Au NPs of achieved by using vibrating ball milling. However, this method produces inhomogeneous size distribution of Au NPs, which limits the practical applications³⁶. Since solid grinding requires a small amount of solvent or does not need any solvent, it would have been highly promising if one could able to synthesize the solid chitosan supported gold NPs in gram-scale through solid-grinding method. This achievement would surely advance their practical applications.

Thus, herein we report an efficient solid-grinding approach for the synthesis of gram-scale quantity of solid chitosan supported gold NPs using sodium borohydride (NaBH₄) reducing agent. Hence, large amount of gold NPs (0.47–12.5 wt %) can be loaded onto the solid chitosan support with gold NPs sizes in the range of 2.8 to 9.5 nm. This solid chitosan supported gold NPs used as heterogeneous catalysts for the oxidative homocoupling of arylboronic acids into biphenyls and the aerobic oxidation of benzyl alcohols into corresponding aldehyde and acids in water under open air. In contrast to conventional solution-based synthesis, solid chitosan supported gold NPs catalysts showed higher activity and selectivity for homocoupling of arylboronic acid reactions. More importantly, the catalytic activity of chitosan-supported nanogold easily modulated by changing the mole ratio of chitosan polymer and gold precursor using the simple solid grinding method. The best of our knowledge, this is the first

report that catalytic activity of hydrophilic polymer supported metal NPs can be tuned/modulated by varying the ratio of the polymer and metal precursor using simple mortar and pestle without the need of solvents.

Results and Discussion

Grinding of white solid chitosan with few microlitres of highly concentrated HAuCl₄ results in the formation of the yellow solid, which was subsequently changed into dark greyish powder by addition of solid NaBH₄, indicating the formation of gold NPs in the solid mixtures. As shown in Table 1, the mole ratio of gold and chitosan polymer (in glucosamine monomer unit) was to be 1:42. This solid mixture was then purified with water using filter paper. It should be mentioned that neither unreduced gold ions nor gold NPs are leached out from the solid chitosan during washing and filtration (Figure S1: ESI). This observation indicates that the reduction of gold ions proceeded quantitatively and the gold NPs are effectively anchored on chitosan polymer. In this synthetic strategy, the process of supporting the gold NPs on the solid chitosan completed within 5–10 minutes, much shorter than 3 to 12 hrs or even a day often required by the solution-based process. More specifically, no solvents are needed; hence, the solubility of hydrophilic polymers, molecular weight and their viscosity problem can in principle be ignored³⁷. In order to verify this, conventional solution approach was used to prepare the chitosan stabilized gold NPs with maintaining the 1:42 mole ratio of gold and chitosan. For example, when the chitosan was dissolved in an aqueous acidic solution and followed by addition of HAuCl₄ and a NaBH₄ a gel formation was occurred (see Figure S2: ESI)³³. Further, it was observed that gold NPs are severally aggregated in the gel. This result clearly reveals that solid-grinding strategy is facile and effective for the direct dispersion of gold NPs on the chitosan polymer support. More loading of catalytically active metals in the form of tiny NPs with greater dispersion onto solid support materials is of

paramount importance for the development high performance metal catalyst³⁸⁻³⁹. Owing to the significant content of primary amines, hydroxyls and esters functional groups in the chitosan polymer, the solid chitosan might function as an excellent platform for loading high density gold NPs without significant aggregations. To investigate whether chitosan would be a superior support material for loading of large amounts of gold NPs, we have prepared different solid chitosan supported gold NPs by changing the mole ratio of chitosan and gold precursor using solid-grinding.

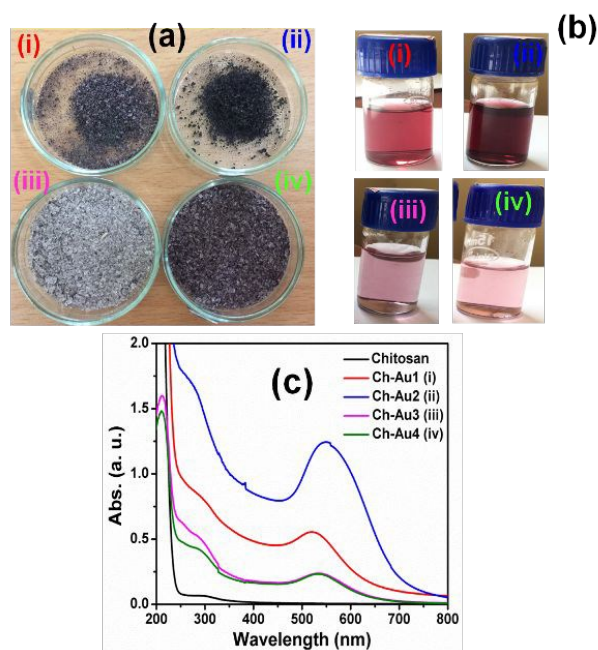


Figure 1. (a) Photographic images of solid chitosan supported gold NPs powder, b) corresponding powders dissolved in 1 % (V/V) aqueous acetic acid solution and their (c). UV-Visible absorption spectra.

As summarized in Table 1; hereafter, the different content of gold NPs supported on chitosan are denoted as Chit-Au1, Chit-Au2, Chit-Au3, and Chit-Au4. The gold content in each solid chitosan was determined using ICP-OES, indicating the gold ions reduced quantitatively and successfully anchored onto the solid chitosan support. Notably, the synthesis of gold NPs supported on solid chitosan using simple mortar and pestle was reproducible for several times (See Figure S3: ESI). Figure 1a shows the photographic images of chitosan supported nanogold powder. Depending on the content of gold and chitosan or vice versa, the color of the solution changes from dark to pale red. The color in the aqueous acidic solutions caused by the light scattering due to surface plasmon resonance band (SPR) of gold NPs⁴⁰. UV-Visible spectra of Figure 1c demonstrate that the wavelength maxima and intensity of the SPR band are highly sensitive to the content of gold and chitosan polymers in the samples. As compared to Chit-Au1, Chit-Au2 exhibit intense SPR band at longer wavelength (550 nm). Though both samples contain same

amount of chitosan support (Table 1), more amount of gold content in chit-Au2 may causes the aggregation of gold NPs on the support, which resulted the shifting of SPR band at longer wavelength than chit-Au1. In contrast, as the amount of chitosan is increased in five times, the SPR peak significantly reduced in Chit-Au3. This result indicating the more content of the chitosan support leads to the high dispersion of gold NPs. when the content of both gold and chitosan increased in the chit-Au4 resulted in narrow SPR band at 525 nm. In order to understand the shifting of SPR band and to investigate the size and morphology of chitosan supported nanogold, high-resolution TEM analysis were performed. As shown in Figures 2a-2d and Figure S4: ESI, the morphology of gold NPs in all four samples exhibits nearly spherical in shapes, and are distributed homogeneously in the chitosan support. This particles exhibits clear diffraction rings in SAED patterns (Figure S4d insert image, ESI), and corresponding to d-spacing of 2.27, 1.96, 1.39 and 1.19 Å for (111), (200), (220) and (311) planes of the fcc structure of metallic gold (JCPDS No. 04-0784)⁴¹⁻⁴³. The size distribution histogram plots were constructed for all four samples by analyzing more than 250 particles from the HRTEM images of corresponding samples and particles sizes were determined to be 5.6 ± 1.5 , 9.5 ± 2.7 , 3.8 ± 1.7 and 2.8 ± 1.7 nm for chit-Au1, chit-Au2, chit-Au3, and chit-Au4, respectively (Figures 2e-2h and Table 1). Both HRTEM images and histogram plots revealed increasing the chitosan support in chit-Au3 and chit-Au4, not only reduce the size of gold NPs but also the particles were greatly dispersed homogeneously without bulk or lumps of aggregations on the solid chitosan support (see Figure S4: ESI). It is reported elsewhere that more amount of stabilizing polymer increases large number of nucleation sites for growth of more number of tiny particles⁴⁴⁻⁴⁵. Because of this high dispersion of smaller gold NPs on the chitosan support, the SPR band was significantly blue shifted in both chit-Au3 and chit-Au4. In contrast to chit-Au1, the bigger sized gold NPs were obtained for chit-Au2. Obviously, the loading of more amounts of gold NPs on less amount of solid support tends to form bigger sized particles due to aggregation that causes the red shifting of SPR band in chit-Au2. It is noteworthy to mention that more loading of metals on solid support materials like metal organic framework and other mesoporous materials leads to formation of rods and wire like structures by aggregation due to weak interaction between metals and support functional groups⁴⁶⁻⁴⁸. In contrast, the multifunctional groups present in the chitosan not only strongly interacting with the gold atoms and also providing a large number of adsorption site for high dispersion of gold NPs. This observation further supports from the FTIR study of chitosan supported gold NPs (Figure S5: ESI). The absorption bands at 1659 cm^{-1} (amide I for C=O vibration), 1598 cm^{-1} (NH_2 bending in primary amines), 1552 cm^{-1} (NH bending in amide II vibration and 3422 cm^{-1} (OH and NH vibration) are slightly shifted with reduced intensities. The shifting of absorption bands with peak intensity reduction compared to free chitosan

can be attributed to the interaction between chitosan and gold NPs⁴⁹⁻⁵⁰. In addition, the peak reduction was very significant in the case of chit-Au2, which is due to the more loading of gold NPs on chitosan support.

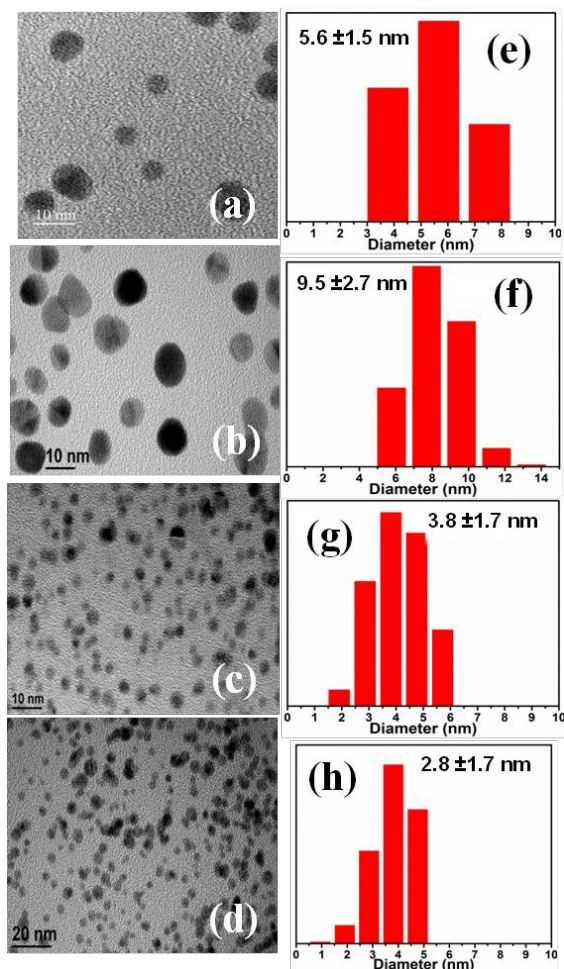


Figure 2. TEM images and corresponding particles size histogram plot (a) & (e) chit-Au1, (b) & (f) chit-Au2, (c) & (g) chit-Au3, and (d) & (h) chit-Au4.

The electronic structure of chitosan supported gold NPs were analyzed by using XPS and XANES. The two peaks are due to spin-orbit coupling of Au4f at 83.7 and 87.9 eV in the XPS spectra (Figure S6b; ESI) ensuring the complete reduction of Au³⁺ to Au(0) occurred during solid-grinding. The reduction of white line intensity at 11923 eV compared to Au foil in the XANES spectra at Au-L3 edge (Figure S7: ESI) is implying the significant reduction of d-holes⁵¹⁻⁵³ in the chitosan supported gold NPs confirming the formation gold NPs in chit-Au1. These results clearly demonstrate that chitosan can be used as superior support materials for both loading of high density of gold NPs as well as the preparation of different sized gold particles using simple solid-grinding.

To determine the available surface area of gold NPs supported on solid chitosan, the Langmuir-adsorption isotherm was used with *P*-nitro thiophenol (PNTPT) as a probe ligand⁵⁴⁻⁵⁵. Various concentrations of PNTPT were mixed with

few milligram of solid chitosan supported gold NPs in aqueous solutions. The mole of adsorbed PNTPT on the gold NPs surface was calculated from a calibration curve using the extinction coefficient of PNTPT (refer ESI)⁵⁵. It should be mentioned that PNTPT adsorb selectively only on gold NPs surface and not on chitosan polymer. As shown in Figure 3, the adsorption isotherm was plotted between the number of moles of adsorbed PNTPT per gram of gold NPs and the equilibrium concentration of PNTPT for four samples to determine the surface area of supported gold NPs. Interestingly, all four samples show the straight line in the adsorption isotherm. Langmuir-isotherm plots were then used to determine the available surface area of gold NPs on the chitosan support.

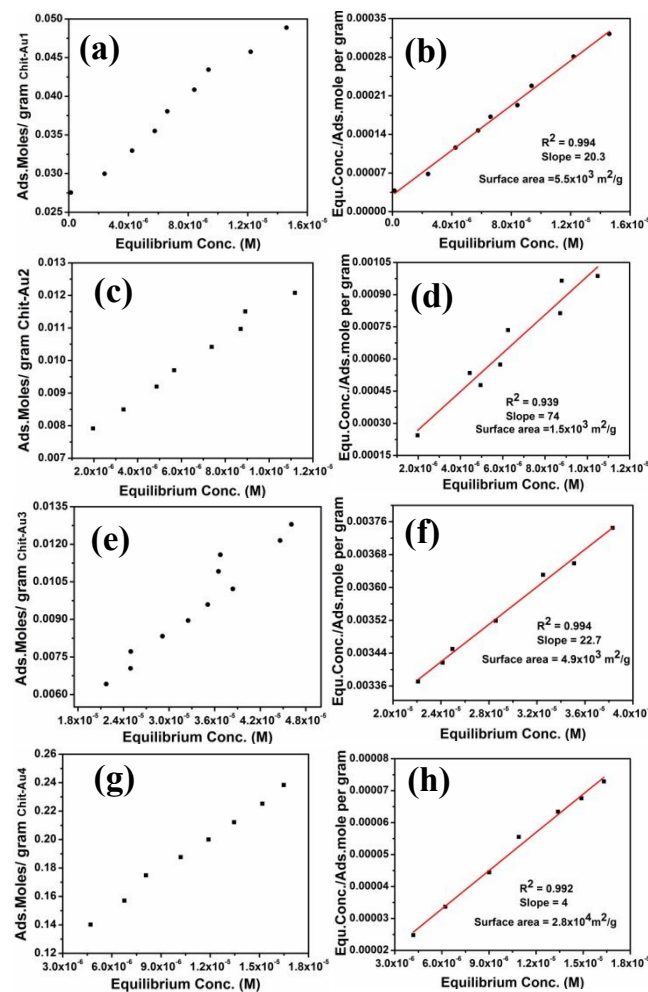


Figure 3. (a), (c), (e), and (g) are adsorption isotherm of PNTPT on Chit-Au1, Chit-Au2, Chit-Au3, and Chit-Au4, (b), (d), (f), and (h) are Langmuir isotherm of the adsorption of PNTPT on the Chit-Au1, Chit-Au2, Chit-Au3, and Chit-Au4, respectively.

Though all four samples have shown higher surface area, the highest surface area *ca.* $2.8 \times 10^4 \text{ m}^2/\text{g}$ was observed only in chit-Au4. This may be due to high dispersion of large number of smaller sized gold NPs on the chitosan support. Compared to chit-Au3, chit-Au1 has showed higher surface area, *ca.*

$5.5 \times 10^3 \text{ m}^2/\text{g}$, even though chit-Au3 has smaller sized gold NPs. Since chit-Au3 contains large amount of chitosan polymer than chit-Au1, either some of the gold NPs may be buried inside the chitosan polymer or the exposed surface atoms at gold NPs may be covered by polymers. Both concomitantly affect the thiol binding at gold NPs surfaces, which in turn reduces the available surface area of gold NPs in chit-Au3. In contrast, the Langmuir-isotherm plots of chit-Au2 have higher slope of 74 g mol^{-1} and the corresponding surface area was found to be much lower than other three samples.

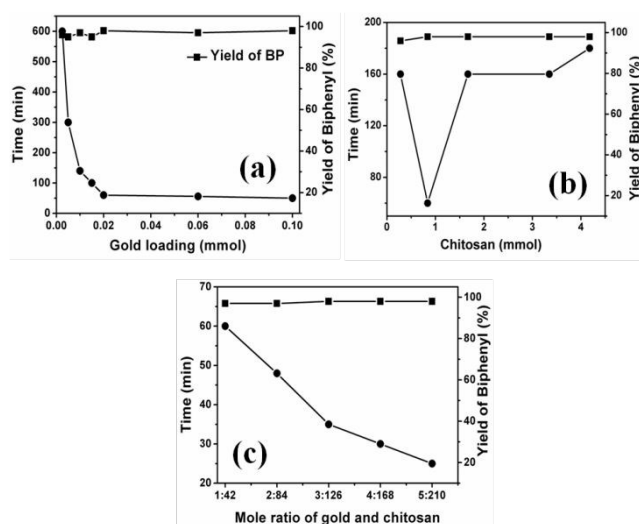


Figure 4. The catalyst optimization in homocoupling of phenylboronic acid. (a) Varying of mole of gold on fixed amount of chitosan support (0.84 mmol in glucosamine monomer unit), (b) varying chitosan support with fixed gold content (0.02 mmol Au) and (c) simultaneously increasing both the content of gold and chitosan.

This result clearly implies that the available surface area of gold NPs supported on solid chitosan not only strongly dependent on the size of gold NPs, but also dependent on the amount of chitosan polymer. Therefore, higher available surface area of supported gold NPs could be easily synthesized in gram scale by simple solid-grinding. Solid-grinding with mortar and pestle using chitosan as a unique support allowed for rapid preparation of supported catalysts with an improved loading efficiency and greater uniformity of gold NPs, which were then employed in the homocoupling of phenylboronic acid in water at room temperature under air (see ESI for reaction details). It is worthy to mention that these solid chitosan supported gold NPs were functioning as heterogeneous catalysts during the reactions. As shown in Figure 4a, while the amount of gold loading increases from 0.0025 to 0.1 mmol on fixed amount of chitosan support (0.84 mmol), the time taken for the complete conversion of phenylboronic acid into biphenyl was reduced sharply indicating the gold NPs supported on solid chitosan actively catalyzing the homocoupling reaction. After 0.02 mmol gold, the reaction time has not reduced sharply and almost constant

even at higher gold content. This result implies that when gold loading exceed more than 0.02 mmol on 0.84 mmol chitosan leads to aggregation of gold NPs, which reduces the total available surface areas and thus decreases the catalytic activity of gold NPs (chit-Au2 details in table 1). To study whether more content of chitosan support have any impact on the catalytic activity of gold NPs, the chitosan support was increased from 0.28 to 4.2 mmol and the amount of gold was kept constant (0.02 mmol Au) during the solid-grinding. As depicted in Figure 4b, when chitosan polymer increased or decreased from 0.84 mmol, the catalytic activity of gold NPs decreases. This could be due to the aggregation of gold NPs might occurs at lesser amount of chitosan or some of the active sites at gold NPs may be partially blocked at higher amount of chitosan polymer. These both concurrently affect the catalytic activity of gold NPs. From these results, 0.02 mmol Au on 0.84 mmol chitosan (1:42 mole ratio of gold and chitosan) was chosen as an optimum catalysts for homocoupling reactions. In order to demonstrate that the solid grinding is facile and promising technique for gram-scale synthesis of chitosan supported nanogold catalysts, both gold and chitosan was increased up to five times with keeping 1:42 mole ratio of gold and chitosan. It is noteworthy to mention that due to high viscous nature of chitosan polymer in aqueous solutions, it is impossible to synthesize the catalytically active chitosan stabilized gold NPs in gram scale using solution based methods (see details in ESI, Table S1). As the amount of gold and chitosan were increased gradually with maintaining 1:42 mole ratio, the catalytic activity of gold NPs was greatly increased (Figure 4c). These results strongly demonstrating the chitosan can be used as excellent support for high loading of gold NPs. Thus, highly active and selective Au NPs catalysts supported on chitosan could be achieved in gram-scale rapidly by using simple mortar-solid grinding, which is not possible in solution-based method.

Table 2. Homocoupling of various *p*-substituted phenylboronic acids catalyzed by solid chitosan supported gold NPs^a.

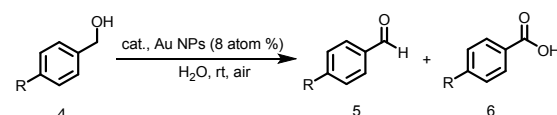
Entry	R	Time (h)	Yield (%) ^b	
			2	3
1	H	1	98	Trace
2	Me	2	99	0
3	OMe	2	95	Trace
4	F	2	97	0
5	Cl	3	97	Trace
6	CN	5	94	Trace

^aReaction conditions: substrate (0.25 mmol), water (15 mL), chitosan 0.84 mmol, and Au (0.02 mmol). ^bIsolated yields

It is interesting to note that solid chitosan supported gold catalysts possess excellent selectivity toward the formation of

biphenyl regardless of the amount of gold and chitosan. As chitosan possesses an excellent matrix to activate the phenylboronic acids into tetra coordinated phenylboronate ester at the gold surfaces, it completely eliminated the use of inorganic bases and increases the selectivity to biphenyl formation^{20,56}. Since all the reactions were carried out in water at pH of 6.5-7.0, only a trace amount of phenol (> 2-3%) formation was observed, which is inevitable due to the formation of superoxide species around gold NPs surfaces^{19,57-58}.

Table 3. Oxidation of various *p*-substituted benzyl alcohols catalyzed by solid chitosan supported gold NPs^a



Entry	R	Time (min)	Yield (%) ^b	
			5	6
1	H	90	0	99
2	OH	25	99	0
3	OMe	5	97	Trace
4	NO ₂	150	0	98
5	1-Indanol	80	99 ^c	-

^aReaction conditions: substrate (0.25 mmol), 300 mol%, K₂CO₃ (0.75 mmol), water (15 mL), chitosan (0.84 mmol), and Au (0.02 mmol). ^bIsolated yields. ^c1-Indanone

To examine the versatility of this chitosan supported nanogold catalysts under an optimized conditions (0.02 mmol Au on 0.84 mmol chitosan), homocoupling reactions involving other *p*-substituted arylboronic acids was tested. Phenylboronic acid possessing electron donating groups such as 4-methyl and 4-methoxy arylboronic acids afforded excellent yields and selectivity into corresponding biphenyl in 2 hrs (entries 2 and 3, Table 2), even though they have taken longer reaction times than phenylboronic acids. Phenylboronic acids with electron-withdrawing 4-fluoro, 4-chloro and 4-cyano substituents (entries 4, 5 and 6, Table 2) gave the corresponding biaryls in 97, 97 and 94% yields and the corresponding phenols in 0, 2 and 6% yields after 2, 3 and 5 hours, respectively. This result demonstrates that this catalyst works very efficient in terms of achieving higher activity and selectivity for both electron donating and withdrawing substituents in the phenylboronic acid.

Encouraged by these results, we are further interested to investigate the potential of solid chitosan supported nanogold catalysts in aerobic oxidation of benzyl alcohols into corresponding aldehydes and acids. Thus, the catalyst was tested for the oxidation of various *p*-substituted benzyl alcohols in aqueous solutions in the presence of 300 mol% K₂CO₃ using molecular oxygen as oxidant. However, solid chitosan supported nanogold applied as heterogeneous catalysts, it works very efficient for oxidation of various *p*-

substituted benzyl alcohols into corresponding aldehyde and acids (Table 3). For example, the oxidation of benzyl alcohol in the presence of the supported gold catalyst gave corresponding acids in 99 % yield after 90 min. Hydroxyl and methoxy substituted benzyl alcohols were oxidized quantitatively into corresponding aldehydes in 25 and 5 minutes (entry 2 and 3, table 3), respectively. In contrast, electron withdrawing substituent of *p*-nitro benzyl alcohol was almost converted into the corresponding acids in 150 min under the same reaction conditions (entry 4, table 3). This experimental result showed that the strong electron donating groups present in the benzyl alcohols not only increase the rate of the oxidation reactions but also exclusively affording to desired aldehyde products. Further, 1-indanol selectively oxidized into 1-indanone in 99 % yield after 80 min (entry 5, table 3).

In a typical solid materials supported metal nanoparticles catalysts, the catalysts recovery and reusability is an important property from economic and industrial point of view. Therefore, the reusability of solid chitosan supported nanogold catalysts was established in both homocoupling of 4-methyl phenylboronic acid and aerobic oxidation of *p*-hydroxyl benzyl alcohols under the optimized reaction conditions as listed in entry 2 (table 2) and entry 2 (table 3). After completion of each homocoupling and alcohol oxidation reaction, the solid catalysts centrifuged, washed with water, dried and successfully reused for five cycles without notable loss of activity and selectivity. As shown in Figure S9: ESI, *p*-methyl phenylboronic acids was exclusively converted into the corresponding biphenyl in excellent yield was observed over the five cycles. On the other hand, the oxidation of *p*-hydroxyl benzyl alcohol gave more selectively into the corresponding aldehydes and the yields over the five cycles were 99, 95, 98, 96 and 94%, respectively. Figure S10: ESI shows the TEM micrograph of recovered catalysts obtained from the homocoupling reaction of *p*-methyl phenylboronic acids after fifth cycles. As can be seen in from these images, the gold NPs were well distributed over the chitosan support without any noticeable aggregations. Therefore, it can be realized that gold NPs on the chitosan support was preserved after fifth cycles. The ICP-OES analysis of the corresponding filtrate showed no gold was leached from the catalyst indicating the gold NPs were effectively anchored on the chitosan support. Next, to study the preparation of solid chitosan supported gold NPs catalysts by physical mixing of gold chloride and NaBH₄ with the chitosan in pestle and mortar exhibits comparable or better catalytic activity as compared to other hydrophilic polymer stabilized gold NPs catalysts synthesis. Hence, other well-known polymers such as PVA and PVP stabilized gold NPs catalysts were prepared using mortar and pestle (refer ESI) and their catalytic activity was tested for homocoupling of phenylboronic acid (entry 1, table 2). It should be mentioned that the 1:42 ratio of gold and PVA / PVP in monomer was maintained during solid grinding. As indicated in entries 2 and

Journal Name

ARTICLE

3 in table 4, PVA and PVP-stabilized gold NPs show inferior catalytic activity toward the homocoupling of phenylboronic acid indicating both PVA and PVP are incapable to stabilize the Au NPs effectively in solid grinding using mortar and pestle (Figure S10 and Table S2; ESI).

View Article Online
DOI: 10.1039/D0NJ04255B

Table 4. Catalytic activity and selectivity comparison toward the homocoupling of phenylboronic acids using solid chitosan supported gold catalyst and other reported gold catalysts synthesized from conventional solution based methods.

Entry	Method	Catalysts	Amount of gold (mmol)	Time (hr)	Yield (%)		ref
					2	3	
1	SG	Chit/ Au	0.005 ^a	5	98	Trace	This work
2	SG	PVA/Au	0.005 ^a	5	ND	ND	See ESI
3	SG	PVP/Au	0.005 ^a	-	ND	ND	See ESI
3	SB	Chit/Au	0.005 ^a	9	93	6	20
4	SB	Starch/Au	0.005 ^a	7	96	4	20
5	SB	PNIPAM/Au	12-36 ^b	2-12	<95	trace	59-60
6	SB	PS-co-PMAA/Au	6.8 ^c	8 ^f	99	-	61
7	SB	PS-PAMAM/Au	0.007 ^d	24	99	-	62
8	SB	PVP/Au	0.005 ^a	15	31	69	20 and 63

SG and SB are solid-grinding and solution based, respectively. ^a, ^b, ^c, and ^d are 0.25, 0.17, 0.24, and 0.5 mmol of phenylboronic acids were used, respectively. ^e– 105 °C used for coupling reaction.

Indeed, the comparative studies between other hydrophilic polymer stabilized gold NPs using conventional solution based methods reported in the literature and chitosan supported gold catalysts obtained from solid-grinding clearly demonstrating the chitosan supported gold NPs works very efficient catalysts in homocoupling of phenylboronic acid. For example, though starch can effectively stabilize the gold NPs, however, it lost their catalytic activity at the end of the coupling reaction due to aggregation. When the same reaction was carried out using PVP-stabilized gold NPs under *quasi-homogeneous* conditions in aqueous acidic solution only 17% of biphenyl product was obtained after 9 hrs. Despite the composite of the PNIPAM/Au system possess interesting thermosensitive property, the present catalytic system shows quite high catalytic activity. This comparative study clearly indicates that chitosan possesses excellent matrix for synthesis of highly efficient and versatile supported gold catalysts in gram-scale using simple mortar and pestle by solid grinding. Further, the deposited gold on solid metal oxides such as TiO₂ and MAO possesses interesting catalytic activities⁶³⁻⁶⁴, however their preparation is more complex and laborious compared to the presents catalysts system. This result further demonstrates that solid grinding with simple mortar and pestle could be used as promising tool to achieve highly efficient heterogeneous metal catalysts.

Conclusions

In conclusion, a facile and sustainable approach was developed for gram-scale synthesis of chitosan supported gold NPs by solid-grinding. Abundant hydroxyl and amine functional groups present in the chitosan polymer allowed for rapid preparation of supported catalysts with an improved loading efficiency and greater uniformity of gold NPs using mortar and

pestle. The supported gold NPs works as efficient heterogeneous catalysts and possesses outstanding activity and selectivity in oxidative homocoupling of phenylboronic acids and aerobic oxidation alcohols in water as greener solvents. The catalytic activity of solid chitosan supported gold NPs can be easily modulated by changing the mole ratio of chitosan polymer and gold precursors. Further, the catalytic activity comparison studies between the other well known hydrophilic polymers stabilized colloidal nanogold catalysts prepared from conventional solution based methods and the present supported gold catalysts indicates that solid chitosan supported gold NPs possess superior catalytic activity and selectivity. Therefore, rapid preparation of biopolymer of chitosan supported gold NPs in gram-scale by simple solid-grinding can inspire more studies on the design and application of the solid polymer supported metal catalysts.

Conflicts of interest

There are no conflicts to declare.

Acknowledgements

AM acknowledges DST-SERB, New Delhi for the award of financial support vide grant No: YSS/2015/001124. We also thank UGC-DAE Consortium for Scientific Research (CSR-IC-ISUM-06/CRS-289/2019-20/1341). Characterization studies acquired from GNR Instrumental facility, University of Madras, Guindy Campus is greatly acknowledged. Thanks to Dr. S. N. Jha, for XANES analysis at Indus-2, RRCAT, India.

Notes and references

- 1 T. Ishida, N. Kinoshita, H. Okatsu, T. Akita, T. Takei, M. Haruta, Influence of the Support and the Size of Gold

- Clusters on Catalytic Activity for Glucose Oxidation, *Angew. Chem. Int. Ed.*, 2008, **47**, 25, 9265-9268.
- 2 L. X. Dien, T. Ishida, A. Taketoshi, Q-D. Truong, H. D. Chinh, T. Honma, T. Murayama, M. Haruta, Supported gold cluster catalysts prepared by solid grinding using a non-volatile organogold complex for low-temperature CO oxidation and the effect of potassium on old particle size, *Appl. Catal. B*, 2019, **241**, 539-547.
 - 3 T. Ishida, M. Nagaoka, T. Akita and M. Haruta, *Chem.-Eur. J.*, 2008, **14**, 8456-8460.
 - 4 L. X. Dien, Q. D. Truong, T. Murayama, H. D. Chinh, A. Taketoshi, I. Honma, M. Haruta, T. Ishida, Gold Nanoparticles Supported on Nb₂O₅ for Low-Temperature CO Oxidation and as Cathode Materials for Li-ion Batteries, *Appl. Catal.*, A, 2020, **603**, 117747.
 - 5 M. Stratakis and H. Garcia, Catalysis by supported gold nanoparticles: beyond aerobic oxidative processes, *Chem. Rev.*, 2012, **112**, 4469-4506.
 - 6 T. Tsukuda, H. Tsunoyama and H. Sakurai, Aerobic Oxidations Catalyzed by Colloidal Nanogold, *Chem. Asian J.*, 2011, **6**, 736-748.
 - 7 Y. Zhang, X. Cui, F. Shi, and Y. Deng, Nano-gold catalysis in fine chemical synthesis, *Chem. Rev.*, 2012, **112**, 2467-2505.
 - 8 J. Garcia-Calvo, V. Garcia-Calvo, S. Vallejos, F. C. Garcia, M. Avella, J. M. Garcia, and T. Torroba, Surface coating by gold nanoparticles on functional polymers: on-demand portable catalysts for Suzuki reactions, *ACS Appl. Mater. Interfaces*, 2016, **8**, 24999-25004.
 - 9 H. Tsunoyama, H. Sakurai, N. Ichikuni, Y. Negishi and T. Tsukuda, Colloidal Gold Nanoparticles as Catalyst for Carbon-Carbon Bond Formation: Application to Aerobic Homocoupling of Phenylboronic Acid in Water *Langmuir*, 2004, **20**, 11293-11296.
 - 10 W. Jang, H. Byun, and J. H. Kim, Encapsulated gold nanoparticles as a reactive quasi-homogeneous catalyst in base-free aerobic homocoupling reactions, *ChemCatChem*, 2020, **12**, 3, 705-709.
 - 11 M. Haruta, Gold rush, *Nature*, 2005, **437**, 7062, 1098-1099.
 - 12 E. Oh, K. Susumu, A. J. Makinen, J. R. Deschamps, A. L. Huston, and I. L. Medintz, Colloidal stability of gold nanoparticles coated with multithiol-poly (ethylene glycol) ligands: importance of structural constraints of the sulfur anchoring groups, *J. Phy. Chem. C*, 2013, **117**, 37, 18947-18956.
 - 13 K. M. Koczkur, S. Mourdikoudis, L. Polavarapu and S. E. Skrabalak, Polyvinylpyrrolidone (PVP) in nanoparticle synthesis, *Dalt. Trans.*, 2015, **44**, 17883-17905.
 - 14 A. Villa, D. Wang, D. S. Su, and L. Prati, Gold sols as catalysts for glycerol oxidation: The role of stabilizer, *ChemCatChem*, 2009, **1**, 4, 510-514.
 - 15 K. Wongmanee, S. Khuanamkam, and S. Chairam, Gold nanoparticles stabilized by starch polymer and their use as catalyst in homocoupling of phenylboronic acid, *Journal of King Saud University - Science*, 2017, **29**, 5, 547-552.
 - 16 L. M. Rossi, J. L. Fiorio, M. A. S. Garcia and C. P. Ferraz, The Role and Fate of Capping Ligands in Colloidally Prepared Metal Nanoparticle Catalysts, *Dalt. Trans.*, 2018, **47**, 5889-5915. DOI: 10.1039/D0NJ04255B
 - 17 J. Van Rie, and W. Thielemans, Cellulose-gold nanoparticle hybrid materials, *Nanoscale*, 2017, **9**, 8525-8554.
 - 18 H. Tsunoyama, N. Ichikuni, H. Sakurai and T. Tsukuda, Effect of Electronic Structures of Au Clusters Stabilized by Poly(N-Vinyl-2-Pyrrolidone) on Aerobic Oxidation Catalysis, *J. Am. Chem. Soc.*, 2009, **131**, 7086-7093.
 - 19 R. N. Dhital, A. Murugadoss and H. Sakurai, Dual Roles of Polyhydroxy Matrices in the Homocoupling of Arylboronic Acids Catalyzed by Gold Nanoclusters under Acidic Conditions, *Chem. Asian J.*, 2012, **7**, 55-59.
 - 20 J. A. Dahl, B. L. S. Maddux, and J. E. Hutchison, Toward greener nanosynthesis, *Chem. Rev.*, 2007, **107**, 6, 2228-2269.
 - 21 T. Tsuzki, Commercial scale production of inorganic nanoparticles, *Int. J. Nanotechnol.*, 2009, **6**, 5-6, 567-578.
 - 22 P. F. M. de Oliveira, R. M. Torresi, F. Emmerling and P. H. C. Camargo, Challenges and opportunities in the bottom-up mechanochemical synthesis of noble metal nanoparticles, *J. Mater. Chem. A*, 2020, **8**, 16114-16141.
 - 23 B. Donoeva and P. E. de Jongh, Colloidal Au catalyst preparation: selective removal of polyvinylpyrrolidone from active Au sites, *ChemCatChem*, 2018, **10**, 989-997.
 - 24 H. Li, J. V. John, S. J. Byeon, M. S. Heo, J. H. Sung, K. H. Kim and I. Kim, Controlled accommodation of metal nanostructures within the matrices of polymer architectures through solution-based synthetic strategies, *Prog. Polym. Sci.*, 2014, **39**, 1878-1907.
 - 25 R. Narayanan, M. A. El-Sayed, Effect of Catalysis on the Stability of Metallic Nanoparticles: Suzuki Reaction Catalyzed by PVP-Palladium Nanoparticles, *J. Am. Chem. Soc.*, 2003, **125**, 27, 8340-8347.
 - 26 S. Haesuwannakij, Y. Yakiyama, and H. Sakurai, Partially Fluoride-Substituted Hydroxyapatite as a Suitable Support for the Gold-Catalyzed Homocoupling of Phenylboronic Acid: An Example of Interface Modification, *ACS Catal.*, 2017, **7**, 4, 2998-3003.
 - 27 Y. Mikami, A. Dhakshinamoorthy, M. Alvaro and H. Garcia, Catalytic Activity of Unsupported Gold Nanoparticles, *Catal. Sci. Technol.*, 2013, **3**, 58-69.
 - 28 L. M. Dias Ribeiro de Sousa Martins, S. A. C. Carabineiro, J. Wang, B. G. M. Rocha, F. J. Maldonado-Hodar and A. J. Latourrette de Oliveira Pombeiro, Supported Gold Nanoparticles as Reusable Catalysts for Oxidation Reactions of Industrial Significance, *ChemCatChem*, 2017, **9**, 1211-1221.
 - 29 Li. Q. Wu, A. P. Gadre, H. Yi, M. J. Kastantin, G. W. Rubloff, W. E. Bentley, G. F. Payne, and R. Ghodssi, Voltage-dependent assembly of the polysaccharide chitosan onto an electrode surface, *Langmuir*, 2002, **18**, 8620-8625.
 - 30 E. I. Rabea, M. E. T. Badawy, C. V. Stevens, G. Smagghe, and W. Steurbaut, Chitosan as antimicrobial agent: applications and mode of action, *Biomacromolecules*, 2003, **4**, 6, 1457-1465.

- 31 A. Murugadoss, and A. Chattopadhyay, A 'green'chitosan–silver nanoparticle composite as a heterogeneous as well as micro-heterogeneous catalyst, *Nanotechnology*, 2018, **19**, 1, 015603.
- 32 M. Lee, B. Y. Chen, and W. Den, Chitosan as a Natural Polymer for Heterogeneous Catalysts Support: A Short Review on Its Applications, *Appl. Sci.*, 2015, **5**, 4, 1272-1283.
- 33 A. Murugadoss and H. Sakurai, Chitosan-Stabilized Gold, Gold-Palladium, and Gold-Platinum Nanoclusters as Efficient Catalysts for Aerobic Oxidation of Alcohols, *J. Mol. Catal. A Chem.*, 2011, **341**, 1-6.
- 34 W. Wang, and H. Cui, Chitosan-luminol reduced gold nanoflowers: from one-pot synthesis to morphology-dependent SPR and chemiluminescence sensing, *J. Phys. Chem. C*, 2008, **112**, 10759-10766.
- 35 A. Murugadoss, N. Kai and H. Sakurai, Synthesis of Bimetallic Gold-Silver Alloy Nanoclusters by Simple Mortar Grinding, *Nanoscale*, 2012, **4**, 1280-1282.
- 36 D. Debnath, S. H. Kim, K. E. Geckeler, The first solid-phase route to fabricate and size-tune gold nanoparticles at room temperature, *J. Mater. Chem.*, 2009, **19**, 8810-8816.
- 37 P. F. M. de Oliveira, J. Quiroz, D. C. de Oliveira and P. H. C. Camargo, A mechano-colloidal approach for the controlled synthesis of metal nanoparticles, *Chem. Commun.*, 2019, **55**, 14267-14270.
- 38 H. Schreyer, R. Eckert, S. Immohr, J. de Bellis, M. Felderhoff, and F. Schuth, . A general process for the direct dry synthesis of supported metal catalysts, *Angew. Chem. Int. Ed.*, 2019, **58**, 11262-11265.
- 39 B. Gole, U. Sanyal and P. Sarathi Mukherjee, A smart approach to achieve an exceptionally high loading of metal nanoparticles supported by functionalized extended frameworks for efficient catalysis, *Chem. Commun.*, 2015, **51**, 4872-4875.
- 40 L. M. Liz-Marzan, M. Giersig, and P. Mulvaney, Synthesis of Nanosized Gold–Silica Core–Shell Particles, *Langmuir*, 1996, **12**, 18, 4329-4335.
- 41 X. B. Qian, W. Peng, Y. B. Shao, and J. H. Huang, Synthesis and visible light-driven photocatalytic hydrogen production, *Int. J. Hydrog. Energy*, 2018, **43**, 4, 2160-2170.
- 42 D. Su, S. Dou, and G. Wang, Gold nanocrystals with variable index facets as highly effective cathode catalysts for lithium–oxygen batteries, *NPG Asia Mater.*, 2015, **7**, 1, e155.
- 43 R. Torres-Mendieta, D. Ventura-Espinosa, S. Sabater, J. Lancis, G. Minguez-Vega, and J. A. Mata, situ decoration of graphene sheets with gold nanoparticles synthesized by pulsed laser ablation in liquids, *Sci. Rep.*, 2016, **6**, 30478.
- 44 A. Q. Zhang, L. J. Cai, L. Sui, D. J. Qian, and M. Chen, Reducing properties of polymers in the synthesis of noble metal nanoparticles, *Polym. Rev.*, 2013, **53**, 2, 240-276.
- 45 X. Xia, Z. Qiang, G. Bass, M. L. Becker and B. D. Vogt, Morphological control of hydrothermally synthesized cobalt oxide particles using poly (vinyl pyrrolidone), *Colloid and Polymer Science*, 2019, **297**, 59-67.
- 46 J. Han, J. Cho, J. C. Kim, and R. Ryoo, Confinement of supported metal catalysts at high loading in the mesopore network of hierarchical zeolites, with access via the microporous windows, *ACS Catal.*, 2018, **8**, 2, 876-879.
- 47 D. Kunwar, S. Zhou, A. DeLaRiva, E. J. Peterson, H. Xiong, X. I. Pereira-Hernandez, S. C. Purdy, R. ter Veen, H. H. Brongersma, J. T. Miller, and H. Hashiguchi, Stabilizing high metal loadings of thermally stable platinum single atoms on an industrial catalyst support, *ACS Catal.*, 2019, **9**, 5, 3978-3990.
- 48 X. Y. Hao, Y. Q. Zhang, J. W. Wang, W. Zhou, C. Zhang, and S. Liu, A novel approach to prepare MCM-41 supported CuO catalyst with high metal loading and dispersion, *Microporous and Mesoporous Materials*, 2006, **88**, 1-3, 38-47.
- 49 A. Regiel-Futrya, M. Kus-Liskiewicz, V. Sebastian, S. Irusta, M. Arruebo, G. Stochel, and A. Kyziol, Development of noncytotoxic chitosan–gold nanocomposites as efficient antibacterial materials, *ACS Appl. Mater. Interfaces*, 2015, **7**, 2, 1087–1099.
- 50 Q. Li, F. Lu, G. Zhou, K. Yu, B. Lu, Y. Xiao, F. Dai, D. Wu, and G. Lan, Silver inlaid with gold nanoparticle/chitosan wound dressing enhances antibacterial activity and porosity, and promotes wound healing, *Biomacromolecules*, 2017, **18**, 3766-3775.
- 51 A. Murugadoss, K. Okumura and H. Sakurai, Bimetallic AuPd Nanocluster Catalysts with Controlled Atomic Gold Distribution for Oxidative Dehydrogenation of Tetralin, *J. Phys. Chem. C*, 2012, **116**, 26776-26783.
- 52 E. K. Gibson, A. M. Beale, C. R. A. Catlow, A. Chutia, D. Gianolio, A. Gould, A. Kroner, K. M. Mohammed, M. Perdjon, S. M. Rogers, and P. P. Wells, Restructuring of AuPd nanoparticles studied by a combined XAFS/DRIFTS approach, *Chem. Mater.*, 2015, **27**, 3714-3720.
- 53 P. Dash, T. Bond, C. Fowler, W. Hou, N. Coombs, and R. W. Scott, Rational design of supported PdAu nanoparticle catalysts from structured nanoparticle precursors, *J. Phys. Chem. C*, 2009, **113**, 12719-12730.
- 54 M. A. Mahmoud, B. Garlyyev, and M. A. El-Sayed, Determining the mechanism of solution metallic nanocatalysis with solid and hollow nanoparticles: homogeneous or heterogeneous, *J. Phys. Chem. C*, 2013, **117**, 21886-21893.
- 55 K. Paul Reddy, K. Jaiswal, B. Satpati, C. Selvaraju and A. Murugadoss, High yield synthesis of branched gold nanoparticles as excellent catalysts for the reduction of nitroarenes, *New J. Chem.*, 2017, **41**, 11250-11257.
- 56 R. N. Dhital, and H. Sakurai, Oxidative Coupling of Organoboron Compounds, *Asian J. Org. Chem*, 2014, **3**, 6, 668.
- 57 S. Karanjit, M. Ehara, and H. Sakurai, Mechanism of the aerobic homocoupling of phenylboronic acid on Au²⁰⁺: A DFT study, *Chem. Asian J.*, 2015, **10**, 2397-2403.
- 58 S. Carrettin, J. Guzman, and A. Corma, Supported gold catalyzes the homocoupling of phenylboronic acid with high

ARTICLE

Journal Name

View Article Online

DOI: 10.1039/D0NJ04255B

- conversion and selectivity, *Angew. Chem. Int. Ed.*, 2005, **44**, 2242-2245.
- 59 P. N. Eyimegwu, J. A. Lartey, and J. H. Kim, Gold-Nanoparticle-Embedded Poly (N-isopropylacrylamide) Microparticles for Selective Quasi-Homogeneous Catalytic Homocoupling Reactions, *ACS Appl. Nano Mater.*, 2019, **2**, 9, 6057-6066.
- 60 W. Jang, H. Byun, and J. H. Kim, Encapsulated gold nanoparticles as a reactive quasi-homogeneous catalyst in base-free aerobic homocoupling reactions, *ChemCatChem*, 2020, **12**, 3, 705-709.
- 61 X. Zhang, H. Zhao, and J. Wang, Recyclable Au (I) Catalyst for Selective Homocoupling of Arylboronic Acids: Significant Enhancement of Nano-Surface Binding for Stability and Catalytic Activity, *J. Nanosci. Nanotechnol.*, 2010, **10**, 5153-5160.
- 62 J. Zheng, S. Lin, X. Zhu, B. Jiang, Z. Yang and Z. Pan, Reductant-directed formation of PS-PAMAM-supported gold nanoparticles for use as highly active and recyclable catalysts for the aerobic oxidation of alcohols and the homocoupling of phenylboronic acids, *Chem. Commun.*, 2012, **48**, 6235-6237.
- 63 Vinsen, Y. Uetake, and H. Sakurai, Selective Oxidative Hydroxylation of Arylboronic Acids by Colloidal Nanogold Catalyzed in Situ Generation of H₂O₂ from Alcohols Under Aerobic Conditions, *Bull. Chem. Soc. Jpn.*, 2020, **93**, 299-301.
- 64 L. Wang, W. Zhang, D. S. Su, X. Meng, F.-S. Xiao, Supported Au nanoparticles as efficient catalysts for aerobic homocoupling of phenylboronic acid, *Chem. Commun.*, 2012, **48**, 5476-5478.
- 65 W. Jang, J. Yun, L. Ludwig, S. G. Jang, J. Y. Bae, H. Byun, J.-H. Kim, Comparative Catalytic Properties of Supported and Encapsulated Gold Nanoparticles in Homocoupling Reactions, *Front. Chem.* 2020, **8**, 834-842.

